Available online at www.sciencedirect.com
SCIENCE DIRECT®
International Journal of Heat and Mass Transfer 49 (2006) 3360–3370
International Journal of HEAT and MASS TRANSFER
www.elsevier.com/locate/ijhmt

Improved milk fouling simulation in a helical triple tube heat exchanger

P.K. Nema [a,*], A.K. Datta [b]

[a] Department of Post Harvest Management, College of Horticulture, JNKVV, Mandsaur 458001, Madhya Pradesh, India
[b] Department of Agricultural and Food Engineering, Indian Institute of Technology, Kharagpur 721302, West Bengal, India

Received 11 November 2005; received in revised form 28 February 2006
Available online 24 May 2006

Abstract

Performance of a dairy heat exchanger declines as milk fouling deposits on the heating surface. It causes an increased resistance to heat flow thereby the milk outlet temperature decreases with increasing fouling thicknesses. Various models have been suggested for the prediction of fouling thickness and milk outlet temperature in a heat exchanger. The present paper describes an improved simulation model for the accurate estimation of fouling thickness and milk outlet temperature. Local fouling factor in terms of the Biot number is used in the work undertaken. Fouling thickness and milk outlet temperature are predicted as a function of time and over the entire length of the heat exchanger. Right from the beginning fouling occurred to a greater extent towards the outlet and with the progress of time the rate of increase of the fouling thickness decreased. The milk outlet temperature decreased with the time as the fouling increased.

Keywords: Milk; Fouling; Model; Simulation; Heat exchanger; UHT

1. Introduction

Milk fouling has been one of the main challenges for researchers [1]. Not only the effect but also its mitigation strategy is an important area of concern. Proper and effective control of milk fouling demands the accurate measurement of its extent i.e. amount, thickness, distribution, etc. A complete and satisfactory mechanism of milk fouling is not yet clear. For online measurement of milk fouling in a processing plant indirect measurements are suitable. Various models have also been suggested for prediction of fouling in a heat exchanger [2–6]. These models are based on different mechanisms of fouling and one of them is the Fryer and Slater model [7,8]. Simulation of milk fouling in a heat exchanger has been described by earlier researchers [7,8]. Some researchers have suggested a computer-based iterative solution for the accurate estimation of heat transfer coefficient [9] and solution to check the drop in milk outlet temperature due to fouling in a tubular heat exchanger [10]. A temperature dependent milk fouling model has been formulated and simulated in a double concentric tube heat exchanger to predict fouling thickness on the heat exchanger surface [11]. A fouling model based on the Fryer and Slater model was developed for double tube heat exchanger [7] and later on modified for a helical triple tube heat exchanger [8]. In all the previous models [11,7,8] simulation was done using 'C' as the programming language. But in the models values of various parameters were taken as constant parameters, whereas most of them are temperature dependent (Table 1). In the same models, values of model constants and heat transfer coefficients were calculated separately and used throughout the simulation as constant. Hence it is required to integrate these as dependent parameters within the programme and a real time estimation of the heat transfer coefficient before the final simulation is carried out. Keeping these points in mind the present work has been taken up to improve upon the simulation of milk fouling in a helical triple tube heat exchanger. The procedure of the simulation model for milk

* Corresponding author. Tel.: +91 7422 222953; fax: +91 7422 242289.
E-mail addresses: pknema_nerist@yahoo.com (P.K. Nema), akd@iitkgp.ac.in (A.K. Datta).

0017-9310/$ - see front matter © 2006 Elsevier Ltd. All rights reserved.
doi:10.1016/j.ijheatmasstransfer.2006.03.021

Nomenclature

A_f	area of flow of working fluid [m^2]
A_{i2}	heat transfer surface area based on inside diameter of middle tube [m^2]
A_{o1}	heat transfer surface area based on outside diameter of innermost tube [m^2]
A_{t1}	constant [m^{-1}]
A_{t2}	constant [m^{-1}]
Bi_{mi}	modified Biot number on outer surface of innermost tube
Bi_{mo}	modified Biot number on inner surface of middle tube
C_{pf}	specific heat of working fluid [J/kg K]
D_c	coil diameter [m]
D_{eq}	equivalent diameter of tube [m]
D_{i1}	inner diameter of innermost tube [m]
D_{i2}	inner diameter of middle tube [m]
D_{o1}	outer diameter of innermost tube [m]
D_{o2}	outer diameter of middle tube [m]
E_i	activation energy on outer surface of innermost tube [J/mol]
E_o	activation energy on inner surface of middle tube [J/mol]
$f(Bi_{mi})$	function of Bi_{mi}
$f(Bi_{mo})$	function of Bi_{mo}
g	acceleration due to gravity [9.81 m/s^2]
h_{c1}	steam/condensate heat transfer coefficient due to innermost tube [W/m^2 K]
h_{c2}	steam/condensate heat transfer coefficient due to outermost tube [W/m^2 K]
h_f	film heat transfer coefficient with fouled layer present [W/m^2 K]
h_f^o	film heat transfer coefficient without fouling [W/m^2 K]
h_m	milk side heat transfer coefficient [W/m^2 K]
i, j	index
k_c	thermal conductivity of condensate [W/m K]
k_d	thermal conductivity of fouled layer [W/m K]
k_{di}	deposition rate constant due to outer surface of innermost tube [s^{-1}]
k_{do}	deposition rate constant due to inner surface of middle tube [s^{-1}]
k_f	thermal conductivity of milk [W/m K]
k_{ri}	removal rate constant due to outer surface of innermost tube [s^{-1}]
k_{ro}	removal rate constant due to inner surface of middle tube [s^{-1}]
k_s	thermal conductivity of stainless steel [W/m K]
L	length of tube [m]
m_f	mass flow rate of process fluid [kg/s]
N	number of nodes
N_{Nu}	Nusselt number
N_{Pr}	Prandtl number
N_{Re}	Reynolds number
N_{Rec}	critical Reynolds number
q	heat transfer rate [W]
q_1	heat transfer rate through innermost tube [W]
q_2	heat transfer rate through middle tube [W]
R	universal gas constant [8.314 J/mol K]
r_{d1}	radius up to fouled layer due to outer surface of innermost tube [m]
r_{d2}	radius up to fouled layer due to inner surface of middle tube [m]
r_{i1}	inner radius of innermost tube in HTTHE [m]
r_{i2}	inner radius of middle tube in HTTHE [m]
r_{o1}	outer radius of innermost tube in HTTHE [m]
r_{o2}	outer radius of middle tube in HTTHE [m]
t	time [s]
T_{bm}	mean temperature of bulk fluid [°C]
T_f	process fluid temperature [°C]
T_{f1}	steam side film temperature in innermost tube [°C]
T_{f2}	steam side film temperature in outermost tube [°C]
T_{i1wall}	temperature of wall at inner side of innermost tube [°C]
T_{in}	inlet temperature of milk in the HTTHE [°C]
T_{o2wall}	temperature of wall at outer side of middle tube [°C]
T_{out}	outlet temperature of milk in the HTTHE [°C]
T_s	temperature of steam [°C]
U_{i2}	overall heat transfer coefficient due to inner surface of middle tube with fouling [W/m^2 K]
U_{i2}^o	overall heat transfer coefficient due to inner surface of middle tube without fouling [W/m^2 K]
U_{o1}	overall heat transfer coefficient due to outer surface of innermost tube with fouling [W/m^2 K]
U_{o1}^o	overall heat transfer coefficient due to outer surface of innermost tube without fouling [W/m^2 K]
v_f	average velocity of process fluid [m/s]

Greek symbols

μ_c	viscosity of condensate at film temperature [Pa s]
$\Delta\alpha$	time interval [s]
ΔT_{lm}	logarithmic mean temperature difference [°C]
δt	finite time interval [s]
δx	finite length of element [m]
ϕ_{mi}	film coefficients and thermal conductivity ratio for outer surface of innermost tube
ϕ_{mo}	film coefficients and thermal conductivity ratio for inner surface of middle tube
ρ_c	density of condensate [kg/m^3]
ρ_f	density of process fluid at mean temperature [kg/m^3]
λ	latent heat of condensation [J/kg]
τ_c	mass flow rate of condensate per unit perimeter [kg/m]

Table 1
Physico-chemical parameters used in the simulation [10]

Parameter	Calculation	Source
Specific heat of milk [J/kg K]	$C_p = 1.68 \times T + 3864.2$	Sahoo (2001)
Viscosity of milk [Pa s]	$\mu = (-0.00445 \times T + 0.947) \times 10^{-3}$	Sahoo (2001)
Thermal conductivity of milk [W/m K]	$\lambda = 0.00133 \times T + 0.539911$	Sahoo (2001)
Milk density [kg/m^3]	$\rho = 1033.7 - 0.2308 \times T - 0.00246 \times T^2$	Sahoo (2001)
Viscosity of condensate [Pa s]	$\mu = (-7.0 \times 10^{-8} \times T^3 + 4.0 \times 10^{-5} \times T^2 0.0089 \times T + 0.8342) \times 10^{-3}$	Sahoo (2001)
Thermal conductivity of condensate [W/m K]	$\lambda = 0.57026 + 0.16899 \times 10^{-2} \times T - 0.60033 \times 10^{-5} \times T^2$	Empirical eq.
Density of condensate [kg/m^3]	$\rho = 1000.76 - 0.12132 \times T - 0.28125 \times 10^{-2} \times T^2$	Empirical eq.
Latent heat of vaporization [J/kg]	$h_{fg} = 2553840.0 - 2938.93 \times T$	Sahoo (2001)
Thermal conductivity of deposit [W/m K]	$\lambda = 3.73 \times \exp(-2.5 \times 10^{-4} \times T) + 0.27$	Delplace and Leuliet (1995)

fouling in a helical triple tube heat exchanger is described here and results are compared with experimental data.

2. Theoretical consideration

A helical triple tube (concentric) heat exchanger as described by [12] was taken up for modeling milk fouling; detailed dimensions are given in Table 2. In the heat exchanger milk flows through the middle annular space and steam flows in the innermost pipe and in the outermost annular space. Thus milk is heated up from both the sides.

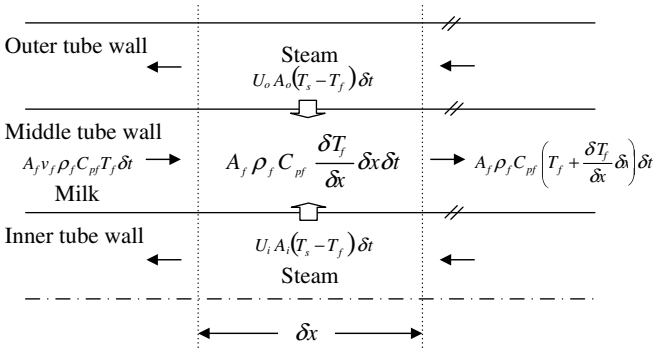

Fig. 1. An element of the heat exchanger showing enthalpy balance.

2.1. Enthalpy balance in the control element

The enthalpy balance is applied on the outer surface of the inner tube and the inner surface of the middle tube, which is shown in Fig. 1. Distribution of fluid, wall and deposit temperatures in a concentric triple tube heat exchanger is shown in Fig. 2.

The enthalpy balance is given by

$$A_f \rho_f v_f C_{pf} \delta t - A_f \rho_f v_f C_{pf} \left(T_f + \frac{\delta T_f}{\delta x} \delta x\right) \delta t + U_{o1} A_{o1} (T_s - T_f) \delta t + U_{i2} A_{i2} (T_s - T_f) \delta t = A_f \rho_f C_{pf} \frac{\delta T_f}{\delta t} \delta x \delta t$$

Simplifying

$$v_f \frac{\delta T_f}{\delta x} + \frac{\delta T_f}{\delta t} = \frac{(U_{o1} A_{t1} + U_{i2} A_{t2})(T_s - T_f)}{\rho_f C_{pf}} \quad (1)$$

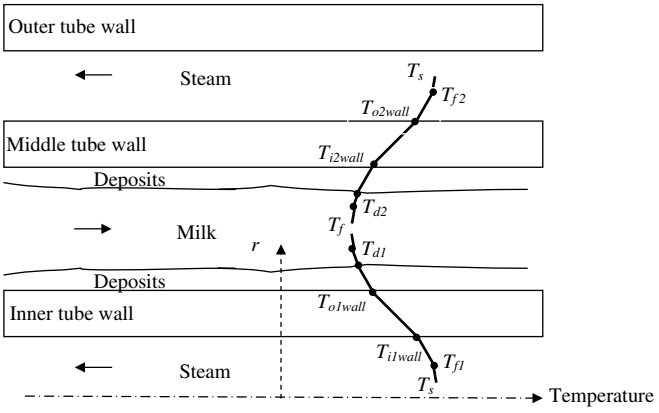

Fig. 2. Distribution of fluid, wall and deposit temperatures in a concentric triple tube heat exchanger.

Table 2
Dimension of UHT milk sterilizer [12]

Heat exchanger dimension			Heating section	Holding section	Cooling section
Diameter [mm]	Innermost tube	Inner	6.0	12.7	9.0
		Outer	8.5	15.0	13.0
	Middle tube	Inner	12.7	–	22.2
		Outer	15.0	–	25.4
	Outermost tube	Inner	22.3	–	–
		Outer	25.4	–	–
Length [m]			2.3	1.0	2.1
Coil diameter [m]			0.3	–	0.3

where,

$$A_{t1} = \frac{A_{o1}}{A_f \delta x} = \frac{2\pi r_{o1}\delta x}{\pi(r_{i2}^2 - r_{o1}^2)\delta x} = \frac{2r_{o1}}{r_{i2}^2 - r_{o1}^2}$$

$$A_{t2} = \frac{A_{i2}}{A_f \delta x} = \frac{2\pi r_{i2}\delta x}{\pi(r_{i2}^2 - r_{o1}^2)\delta x} = \frac{2r_{i2}}{r_{i2}^2 - r_{o1}^2}$$

Fluid temperature is expressed in partial differential form by Eq. (1) which is used in the model. Heat transfer rate is calculated by

$$q = m_f C_{pf}(T_{out} - T_{in}) \tag{2}$$

Based on the overall heat transfer coefficient q can also be obtained by

$$q = (q_1 + q_2) = (U_{o1}A_{o1} + U_{i2}A_{i2})\Delta T_{lm} \tag{3}$$

2.2. Evaluation of heat transfer coefficients of the process fluid

When a fluid flows in the annular region of tubes, the fluid side convection heat transfer coefficient can be calculated under turbulent flow conditions by the following equation [13]:

$$N_{Nu} = 0.027 N_{Re}^{0.8} N_{Pr}^{0.33} \left(\frac{D_{i2}}{D_{o1}}\right)^{0.53} \tag{4}$$

To get the fluid-side heat transfer coefficient of a helical triple tube heat exchanger, Eq. (4) should be modified [14] by multiplying a factor of $\left[1 + 3.5\left(\frac{D_{eq}}{D_c}\right)\right]$. The modified equation can be written as

$$h_f = \left(\frac{k_f}{D_{eq}}\right) 0.027 N_{Re}^{0.8} N_{Pr}^{0.33} \left(\frac{D_{i2}}{D_{o1}}\right)^{0.53} \left[1 + 3.5\left(\frac{D_{eq}}{D_c}\right)\right] \tag{5}$$

Eq. (5) is valid for $N_{Re} \geqslant N_{Rec}$ and $7 < N_{Pr} < 700$ [15].

2.3. Evaluation of condensate heat transfer coefficients

Based on the assumption that the flow of the condensate is laminar i.e. $\frac{2\tau_c}{\mu_c} < 1.2 \times 10^3$ and k_c, ρ_c and μ_c are estimated at the film temperature, the condensate heat transfer coefficients can be obtained from the following equations [16]:

$$h_{c1} = 0.5754 \left[\frac{k_c^3 \rho_c^2 g\lambda}{\mu_c D_{i1}(T_s - T_{i1wall})}\right]^{0.25} \quad \text{and} \tag{6}$$

$$h_{c2} = 0.7250 \left[\frac{k_c^3 \rho_c^2 g\lambda}{\mu_c D_{o2}(T_s - T_{o2wall})}\right]^{0.25} \tag{7}$$

All the properties in the above equations are taken at the film temperature, which are initially assumed as:

$$T_{f1} = T_s - 0.75(T_s - T_{i1wall}) \quad \text{and} \tag{8}$$

$$T_{f2} = T_s - 0.75(T_s - T_{o2wall}) \tag{9}$$

Based on the principle of the heat flux equivalence concept, new wall temperatures are calculated by the following equations:

$$\frac{T_s - T_{i1wall}}{\frac{1}{h_{c1}D_{i1}}} = \frac{T_{i1wall} - T_{bm}}{\frac{\ln\left(\frac{D_{o1}}{D_{i1}}\right)}{2k_s} + \frac{1}{h_m D_{o1}}} \quad \text{and} \tag{10}$$

$$\frac{T_s - T_{o2wall}}{\frac{1}{h_{c2}D_{o2}}} = \frac{T_{o2wall} - T_{bm}}{\frac{\ln\left(\frac{D_{o2}}{D_{i2}}\right)}{2k_s} + \frac{1}{h_m D_{i2}}} \tag{11}$$

2.4. Evaluation of overall heat transfer coefficients

To calculate overall heat transfer coefficients, the following equations are used based on conduction and convention in cylindrical co-ordinates:

$$U_{o1} = \left(\frac{1}{h_f} + \frac{D_{o1}\ln\frac{D_{o1}}{D_{i1}}}{2k_s} + \frac{D_{o1}}{h_{c1}D_{i1}}\right)^{-1} \quad \text{and} \tag{12}$$

$$U_{i2} = \left(\frac{1}{h_f} + \frac{D_{i2}\ln\frac{D_{o2}}{D_{i2}}}{2k_s} + \frac{D_{i2}}{h_{c2}D_{o2}}\right)^{-1} \tag{13}$$

2.5. Heat transfer equations for HTTHE

(i) Without fouling, the outside surface of the inner tube

$$T_s - T_f = \frac{q_1}{h_f^o A_{i1}} \left[\frac{h_f^o}{h_{c1}} + \frac{h_f^o r_{i1}\ln\left(\frac{r_{o1}}{r_{i1}}\right)}{k_s} + \frac{r_{i1}}{r_{o1}}\right] \tag{14}$$

$$\phi_{mi} = \frac{h_f^o}{h_{c1}} + \frac{h_f^o r_{i1}\ln\left(\frac{r_{o1}}{r_{i1}}\right)}{k_s} \tag{15}$$

$$q_1 = U_{o1}^o A_{o1}(T_s - T_f) \tag{16}$$

$$\frac{1}{U_{o1}^o} = \frac{1}{h_f^o}\left[\phi_{mi}\frac{r_{o1}}{r_{i1}} + 1\right] \tag{17}$$

(ii) With fouling, the outside surface of the inner tube

$$T_s - T_f = \frac{q_1}{h_f^o A_{i1}} \left[\frac{h_f^o}{h_{c1}} + \frac{h_f^o r_{i1}\ln\left(\frac{r_{o1}}{r_{i1}}\right)}{k_s} + \frac{h_f^o r_{i1}\ln\left(\frac{r_{d1}}{r_{o1}}\right)}{k_d} + \frac{r_{i1}}{r_{d1}}\frac{h_f^o}{h_f}\right] \tag{18}$$

$$q_1 = U_{o1}A_{o1}(T_s - T_f) \tag{19}$$

and

$$Bi_{mi} = \frac{h_f^o r_{o1}\ln\left(\frac{r_{d1}}{r_{o1}}\right)}{k_d}$$

$$\frac{1}{U_{o1}} = \frac{1}{U_{o1}^o} + \frac{1}{h_f^o}\frac{r_{o1}}{r_{i1}}\left[\frac{r_{i1}}{r_{o1}}(Bi_{mi} - 1) + \frac{h_f^o}{h_f}\frac{r_{i1}}{r_{d1}}\right] \tag{20}$$

(iii) Without fouling, the inside surface of the middle tube

$$T_s - T_f = \frac{q_2}{h_f^o A_{o2}}\left[\frac{h_f^o}{h_{c2}} + \frac{h_f^o r_{o2}\ln\left(\frac{r_{o2}}{r_{i2}}\right)}{k_s} + \frac{r_{o2}}{r_{i2}}\right] \tag{21}$$

Putting,

$$\phi_{mo} = \frac{h_f^o}{h_{c2}} + \frac{h_f^o r_{o2}\ln\left(\frac{r_{o2}}{r_{i2}}\right)}{k_s} \tag{22}$$

and

$$q_2 = U_{i2}^o A_{i2}(T_s - T_f) \tag{23}$$

Then,

$$\frac{1}{U_{i2}^o} = \frac{1}{h_f^o}\left[\phi_{mo}\frac{r_{i2}}{r_{o2}} + 1\right] \tag{24}$$

(iv) With fouling, the inside surface of the middle tube

$$T_s - T_f = \frac{q_2}{h_f^o A_{o2}}\left[\frac{h_f^o}{h_{c2}} + \frac{h_f^o r_{o2}\ln\left(\frac{r_{o2}}{r_{i2}}\right)}{k_s} + \frac{h_f^o r_{o2}\ln\left(\frac{r_{i2}}{r_{d2}}\right)}{k_d} + \frac{r_{i2}h_f^o}{r_{d2}h_f}\right] \tag{25}$$

Using

$$q_2 = U_{i2}A_{i2}(T_s - T_f) \tag{26}$$

and

$$Bi_{mo} = \frac{h_f^o r_{i2}\ln\left(\frac{r_{i2}}{r_{d2}}\right)}{k_d}$$

we get

$$\frac{1}{U_{i2}} = \frac{1}{U_{i2}^o} + \frac{1}{h_f^o}\frac{r_{i2}}{r_{o2}}\left[\frac{r_{o2}}{r_{i2}}(Bi_{mo} - 1) + \frac{h_f^o}{h_f}\frac{r_{i2}}{r_{d2}}\right] \tag{27}$$

Substituting $\frac{r_{i1}}{r_{o1}}(Bi_{mi} - 1) + \frac{h_f^o}{h_f}\frac{r_{i1}}{r_{d1}}$, with $f(Bi_{mi})$; the equation becomes

$$\frac{1}{U_{i2}} = \frac{1}{U_{i2}^o} + \frac{f(Bi_{mo})}{h_f^o}\frac{r_{i2}}{r_{o2}}$$

or,

$$\frac{1}{U_{i2}} = \frac{h_f^o + U_{i2}^o f(Bi_{mo})\left(\frac{r_{i2}}{r_{o2}}\right)}{h_f^o U_{i2}^o}$$

or,

$$U_{i2} = \frac{h_f^o U_{i2}^o}{h_f^o + f(Bi_{mo})\left(\frac{r_{i2}}{r_{o2}}\right)U_{i2}^o}$$

Similarly, substituting $\frac{r_{o2}}{r_{i2}}(Bi_{mo} - 1) + \frac{h_f^o}{h_f}\frac{r_{i2}}{r_{d2}}$ with $f(Bi_{mo})$; from Eq. (20), we get

$$U_{o1} = \frac{h_f^o U_{o1}^o}{h_f^o + U_{o1}^o f(Bi_{mi})\frac{r_{o1}}{r_{i1}}} \tag{28}$$

where $f(Bi_{mi})$ and $f(Bi_{mo})$ are functions of Bi_{mi} and Bi_{mo}, respectively.

Using the characteristic technique as described by Acrivos [17], Eq. (1), a partial differential equation can be converted to an ordinary differential equation. The ordinary differential form of Eq. (1) is

$$\frac{dT_f}{dt} = 2\left[\frac{r_{o1}U_{o1}^o h_f^o}{h_f^o + U_{o1}^o f(Bi_{mi})\frac{r_{o1}}{r_{i1}}} + \frac{r_{i2}U_{i2}^o h_f^o}{h_f^o + U_{i2}^o f(Bi_{mo})\frac{r_{i2}}{r_{o2}}}\right]\frac{T_s - T_f}{(r_{i2}^2 - r_{o1}^2)\rho_f C_{pf}} \tag{29}$$

2.6. Fouling model for a helical triple tube UHT milk sterilizer

For developing the model for fouling in a helical triple tube UHT milk sterilizer, a model as suggested by Fryer and Slater [18] for a tubular heat exchanger was used with suitable modifications. The basic equations used for deposition rate and description of the modification made in the aforesaid model are as follows:

$$\frac{dBi_{mi}}{dt} = k_{di}\exp\left[-\frac{E_i}{RT_{fi}}\right] - k_{ri}Bi_{mi} \tag{30}$$

$$Bi_{mi} = \frac{h_f^o r_{o1}\ln\left(\frac{r_{d1}}{r_{o1}}\right)}{k_d} \tag{31}$$

$$\frac{dBi_{mo}}{dt} = k_{do}\exp\left[-\frac{E_o}{RT_{fo}}\right] - k_{ro}Bi_{mo} \tag{32}$$

$$Bi_{mo} = \frac{h_f^o r_{i2}\ln\left(\frac{r_{i2}}{r_{d2}}\right)}{k_d} \tag{33}$$

2.7. Formulation of the local fouling rate model

Based on the principle of the heat flux equivalence concept T_{fi} is substituted in Eq. (30), then the local overall rate of solid accumulation on the outer surface of the inner tube can be represented as

$$\frac{dBi_{mi}}{dt} = k_{di}\exp\left[-\frac{E}{R}\frac{\left(\phi_{mi} + f(Bi_{mi}) + \frac{r_{i1}}{r_{o1}}\right)}{(T_s + 273)(f(Bi_{mi}) + \frac{r_{i1}}{r_{o1}}) + [(T_f + 273)\phi_{mi}]}\right] - k_{ri}Bi_{mi} \tag{34}$$

Similarly, the local overall rate of solid accumulation on the inner surface of the middle tube can be represented as given below:

$$\frac{dBi_{mo}}{dt} = k_{do}\exp\left[-\frac{E}{R}\frac{\left(\phi_{mo} + f(Bi_{mo}) + \frac{r_{o2}}{r_{i2}}\right)}{(T_s + 273)(f(Bi_{mo}) + \frac{r_{o2}}{r_{i2}}) + [(T_f + 273)\phi_{mo}]}\right] - k_{ro}Bi_{mo} \tag{35}$$

2.8. Determination of activation energy, deposition and removal rate constant

During the initial fouling period, the rate of removal is almost negligible. Therefore, the net rate of fouling is only

due to the rate of deposition [18]. Thus it can be assumed for the initial period only

$$k_{ri}Bi_{mi} \to 0 \quad \text{and} \quad k_{ro}Bi_{mo} \to 0$$

The Arrhenius plot of the initial fouling rate can be shown for the outer surface of the inner tube of a heat exchanger by the expression

$$\frac{dBi_{mi}}{dt} = k_{di}.\exp\left(\frac{-E}{RT_{d1}}\right) \tag{36}$$

or,

$$\begin{aligned}\ln\left(\frac{dBi_{mi}}{dt}\right) &= \ln k_{di} - \frac{E}{RT_{d1}} \\ -\ln\left(\frac{dBi_{mi}}{dt}\right) &= \frac{E}{RT_{d1}} - \ln k_{di}\end{aligned} \tag{37}$$

Plotting $-\ln\left(\frac{dBi_{mi}}{dt}\right)$ vs $\frac{1}{RT_{d1}}$, activation energy (E_i) and deposit rate constant on the outer surface of the inner tube (k_{di}) can be evaluated from the slope and intersect of the plot, respectively.

Similarly the expression for the inner surface of the middle tube can be shown as

$$-\ln\left(\frac{dBi_{mo}}{dt}\right) = \frac{E}{RT_{d2}} - \ln k_{do} \tag{38}$$

Plotting $-\ln\left(\frac{dBi_{mo}}{dt}\right)$ vs $\frac{1}{RT_{d2}}$, activation energy (E_o) and deposit rate constant on the inner surface of middle tube (k_{do}) can be evaluated from the slope and intersect of the plot, respectively.

After a long time when an equilibrium or stable Biot number has been attained, the deposition rate becomes equal to the removal rate on the fluid side of heat exchanger surface. It can be written at this point: $\frac{dBi_{mi}}{dt} = 0$ and $\frac{dBi_{mo}}{dt} = 0$. Hence Eqs. (30) and (32) can be reduced to

$$\begin{aligned}k_{di}\exp\left(-\frac{E_i}{RT_{d1}}\right) &= k_{ri}Bi_{mi\infty} \\ k_{ri} &= \frac{k_{di}}{Bi_{mi\infty}}\exp\left(-\frac{E_i}{RT_{d1}}\right)\end{aligned} \tag{39}$$

and similarly,

$$k_{ro} = \frac{k_{do}}{Bi_{mo\infty}}\exp\left(-\frac{E_o}{RT_{d2}}\right) \tag{40}$$

2.9. Numerical procedure

The number of nodes 'N' along α-characteristics was selected. The temporal separation of nodes along α-characteristics were thus set [11].

$$\Delta\alpha = \frac{L}{N-1}.\frac{1}{v_f} \tag{41}$$

Values of Biot numbers, T_f and T_s are known at certain nodes corresponding to the initial conditions and boundary values.

(i) Initial conditions

$$Bi_{mi}(i,0) = 0, \quad \text{for } i = 1,2,3,\ldots N$$
$$Bi_{mo}(i,0) = 0, \quad \text{for } i = 1,2,3,\ldots N$$

(ii) Boundary conditions

Tube side fluid temperature $T_f(i,j)$ is defined for each simulation. Integration of Eqs. (29), (34) and (35) using the Modified Euler's technique gives

$$T_f(i+1/2,j) = T_f(i,j) + \left.\frac{dT_f}{dt}\right|_{(i,j)}\frac{\Delta\alpha}{2} \tag{42}$$

$$Bi_{mo}(i,j+1/2) = Bi_{mo}(i,j) + \left.\frac{dBi_{mo}}{dt}\right|_{(i,j)}\frac{\Delta\alpha}{2} \tag{43}$$

$$Bi_{mi}(i,j+1/2) = Bi_{mi}(i,j) + \left.\frac{dBi_{mi}}{dt}\right|_{(i,j)}\frac{\Delta\alpha}{2} \tag{44}$$

$$T_f(i+1,j) = T_f(i,j) + \left.\frac{dT_f}{dt}\right|_{(i+1/2,j)}\Delta\alpha \tag{45}$$

$$Bi_{mo}(i,j+1) = Bi_{mo}(i,j) + \left.\frac{dBi_{mo}}{dt}\right|_{(i,j+1/2)}\Delta\alpha \tag{46}$$

$$Bi_{mi}(i,j+1) = Bi_{mi}(i,j) + \left.\frac{dBi_{mi}}{dt}\right|_{(i,j+1/2)}\Delta\alpha \tag{47}$$

3. Experimental fouling

An experiment was conducted on a helical triple tube UHT milk sterilizer. Milk was preheated to 93 °C in a steam-jacketed pan and supplied to the inlet of a heat exchanger by means of a centrifugal pump. Increase in the temperature and a pressure drop were recorded for 75 min of operation. These results were then used to validate the simulated results.

4. Fouling simulation procedure

Milk fouling simulation was carried out to study the fouling behaviour of milk on both surfaces of the helical triple tube UHT sterilizer along its length with time and temperature. The heat transfer coefficients were determined as shown in Fig. 3. The local fouling rate model (Eq. (1)) was derived based on the Kern and Seaton model [18]. It was modified for a helical triple tube heat exchanger. Then overall heat transfer coefficients were derived under fouling and non-fouling conditions. By means of an enthalpy balance on a control volume of the heating section, the change in temperature with time was derived in a partial differential equation form. Then using a characteristics technique as described by Acrivos [17] and application shown by Fryer and Slater [18,19], the partial differential equations were converted to ordinary differential equations. Integration of these constitutive equations were performed by a modified Euler's technique [7]. The values of the Biot

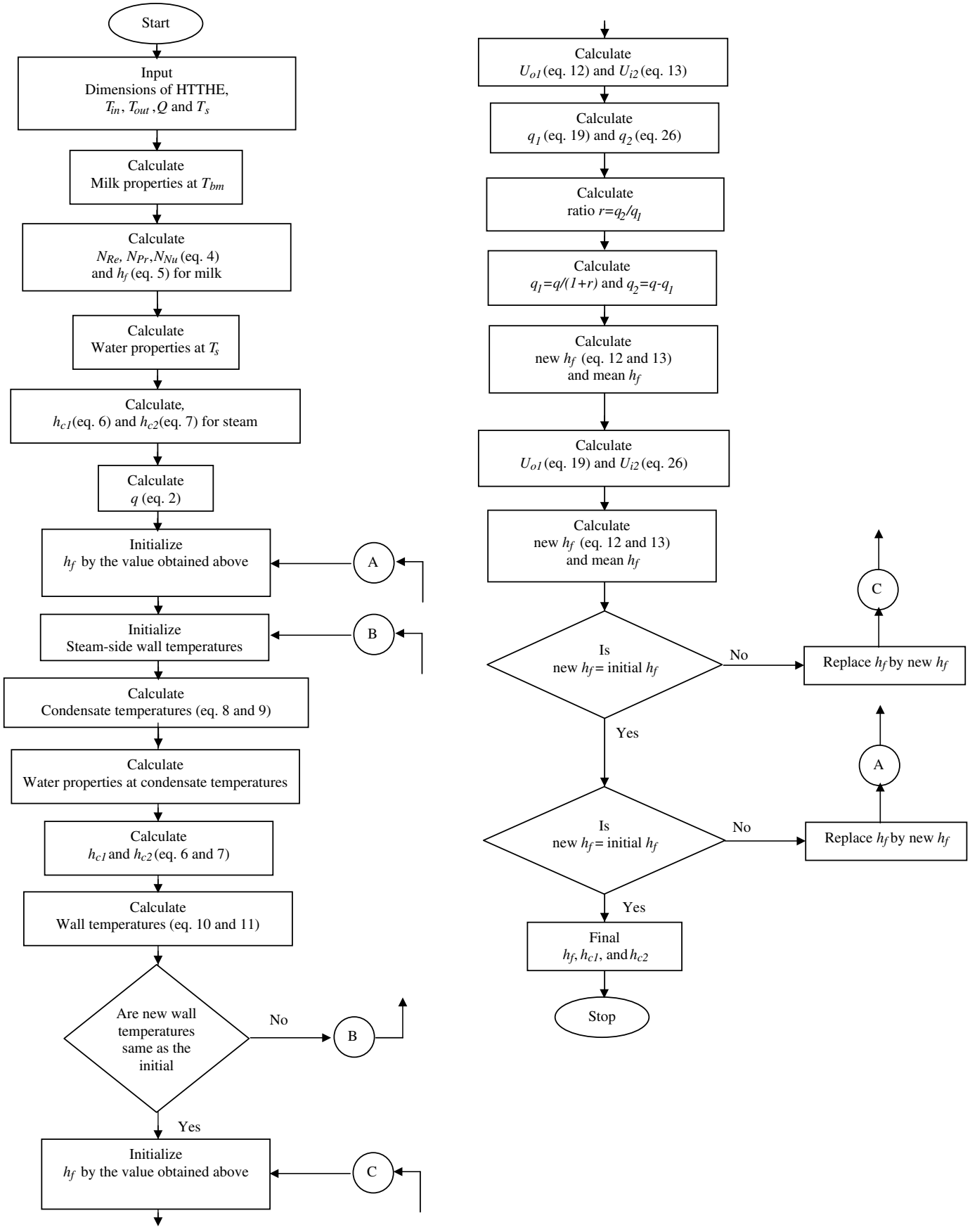

Fig. 3. Flow chart of computer simulation for estimation of heat transfer coefficients.

number and fouling deposits on the outer surface of the inner tube (Bi_{mi} and δ_i) and on the inner surface of the middle tube (Bi_{mo} and δ_o) were obtained at selected nodes along the length of the heat exchanger at different processing times.

A computer programme was written in 'C' to simulate the milk outlet temperature (Fig. 4). After the milk outlet temperature is simulated, the fouling thickness is determined based on the enthalpy balance and assuming a constant heat flux across the heat exchanger wall.

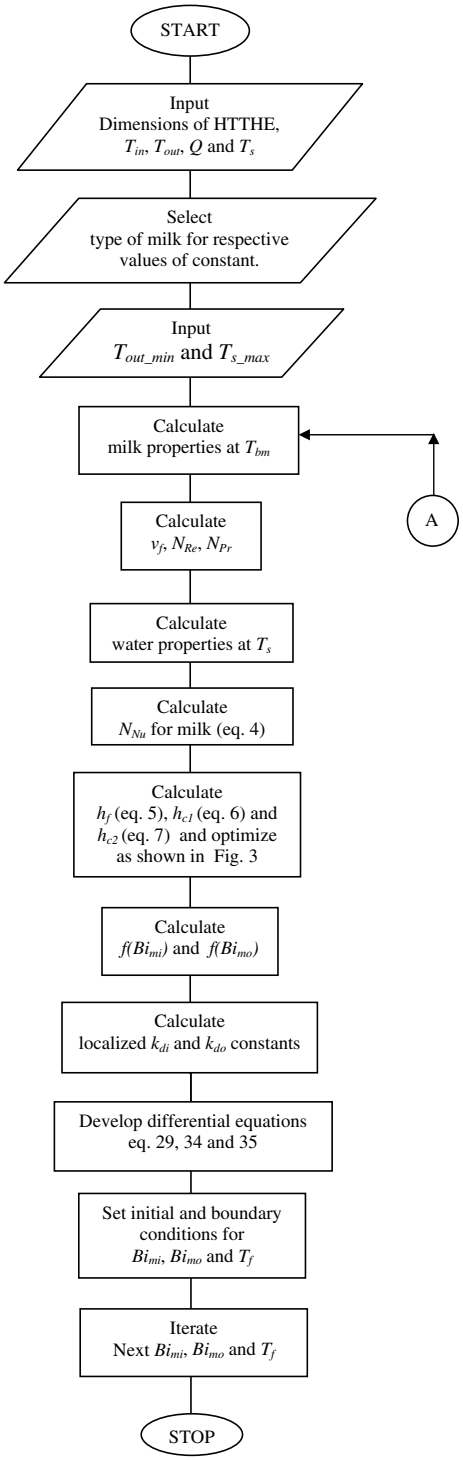

Fig. 4. Flow chart of computer simulation model for estimation of milk fouling.

5. Model input

The physico-chemical parameters, used in this work, can be calculated from different equations as presented in Table 1.

6. Simulation results and discussion

The modified Euler's technique was applied to solve Eqs. (29), (34) and (35). In the 2.28 m long heat exchanger, nodes are selected at intervals of 0.05 m, so there are total 46 nodes. The number of nodes can be changed, but it should not be too small to cause a large deviation from actual values of the model output. Thereafter the number of iterations was calculated by dividing the total time of processing by the time required by milk to travel the whole length of the heat exchanger. Then using Eqs. (42)–(47), milk outlet temperature (T_f), Biot Numbers (Bi_{mi} and Bi_{mo}) and fouling deposits (δ_i and δ_o) were simulated at the selected nodes along the length of helical triple tube heat exchanger.

From Fig. 5, it is evident that the temperature increases along the length of the heat exchanger towards the outlet. With the progress of time, the temperature drops gradually at the respective nodes along the length of the heat exchanger. This is due to the occurrence of fouling. From simulation a constant outlet temperature of 133 °C was found after 75 min. It means that at this point the rate of solid deposition is equal to the rate of solid removal. In the experiment a constant outlet temperature of 129 °C was found after 75 min. The error is of 4 °C, which is higher than the observed value in the experiment. This error is due to the fact that in the model thermal conductivity of deposits has been taken as constant, whereas it changes with temperature and in the model the loss of heat to the surroundings is assumed to be negligible which is very difficult to achieve in practice. Results of the previous model also show the same trend but give a constant milk outlet

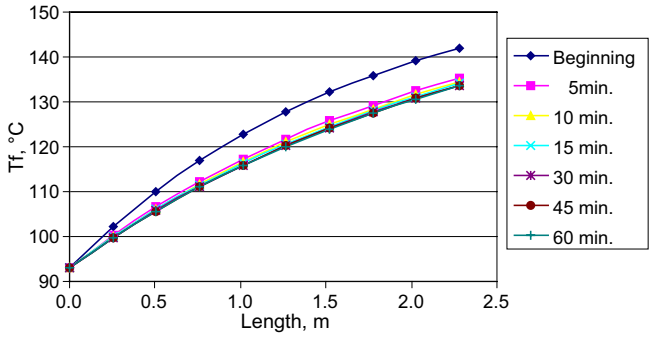

Fig. 5. Variation of temperature along the length of the HTTHE with time of operation.

temperature of about 120 °C after 75 min. So the present model prediction of temperature is comparable with that of experimental results, more justified and therefore acceptable.

From the simulated results as shown in Fig. 6, it is found that the fouling deposits on the outer surface of the inner tube δ_i increases with time. Right from the beginning, the occurrence of fouling deposit is found to be more at the outlet than at the inlet of the heat exchanger; at the same time an increase in fouling is not uniform along the length of the heat exchanger but is asymptotic in nature. These results differ from the previous model's [8] result where a constant fouling thickness was simulated over the whole length of the tube for about an initial 30 min of simulation (Figs. 7 and 8). The temperature of the interface (i.e. T_{d1} and T_{d2}) between the fouling deposit and the bulk fluid is responsible for the occurrence of fouling. In the early stage of operation, as T_{d1} and T_{d2} are equivalent to the constant wall temperature of the heat exchanger, a uniform distribution of the fouling deposit should have occurred throughout the length of the heat exchanger. But the bulk fluid temperature increases as it moves in the tube; an increase in temperature makes protein and other depositable components of milk available in aggregated form and hence causes more deposition towards the outlet. After some time (i.e. beyond 30 min), T_{d1} and T_{d2} approach towards the bulk fluid temperature and because some deposition has already taken place, the rate of further increase in the fouling thickness decreases and hence less and less deposition thickness is added afterwards.

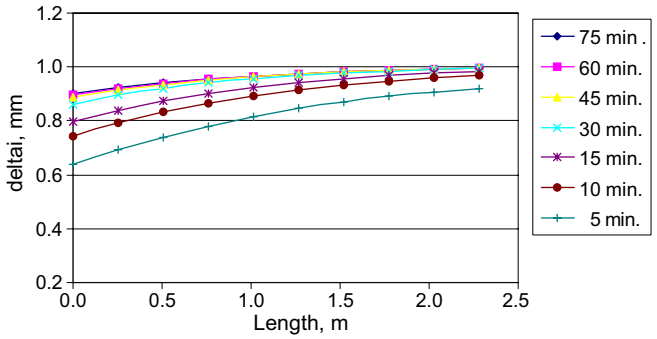

Fig. 6. Variation of fouling deposit on the outer surface of inner tube along the length of the heat exchanger with time.

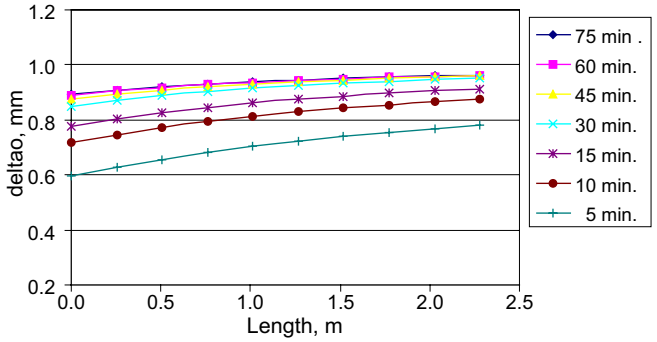

Fig. 7. Variation of fouling deposit on the inner surface of middle tube along the length of the heat exchanger with time.

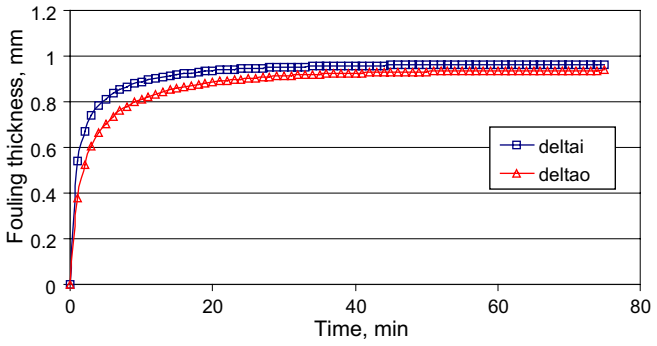

Fig. 8. Variation of average fouling deposit with time.

Fig. 7 shows the increase of the fouling deposit on the inner surface of the middle tube δ_o along the heat exchanger length with time. The nature of the fouling deposit along the length of the heat exchanger is similar to that obtained on the outer surface of the inner tube.

Fig. 8 shows the variation of average fouling deposits for both the outer surface of the inner tube δ_i and the inner surface of the middle tube δ_o with time. The trend of average fouling deposit vs time is asymptotic in nature. The average constant fouling deposit on the outer surface of the inner tube and that on the inner surface of the middle tube are found to be 0.9634 mm and 0.9379 mm, respectively, after 75 min and becomes almost constant thereafter. The previous model [8] gave a stable fouling thickness of about 0.65 mm and 0.74 mm on the outer surface of the inner tube and that on the inner surface of the middle tube, respectively, after 105 min, which is again under prediction of the average fouling thickness as compared to the experimental value (average fouling thickness: 0.76 mm).

With the progress of time, as the fouling deposit increases, the flow area available for the process fluid narrows down. The velocity of the process fluid increases, which leads to an increase in the shear force. So the rate of deposit becomes the same as the rate of removal after a certain time due to the fluid shear forces, which means that fouling stabilizes after 75 min since no appreciable deposit occurs after that time. In the case of modeled data of fouling thickness it is on the higher side because in the actual condition after a certain time the fouling deposition thickness does not increase but it starts to be more compact, whereas in the case of modeling this factor was not taken into consideration. Further work in this area may be required before a definite conclusion can be made on this point. Here it can be concluded that the fouling thickness simulated is on the higher side and it will be less in the actual condition, and one of the factor which may affect it is the rate of change of thermo-physical properties of fouling deposits (i.e. density, thermal conductivity etc.). In this

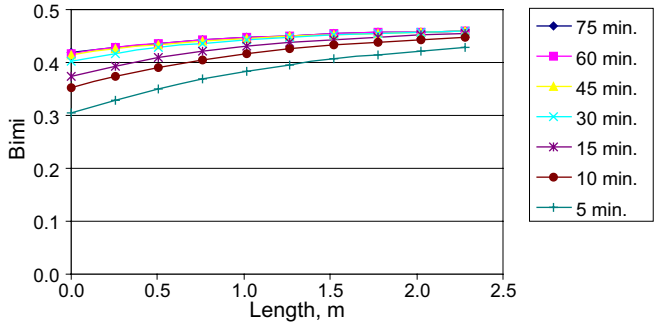

Fig. 9. Variation of Biot number on the outer surface on inner tube along the length of the HTTHE with time.

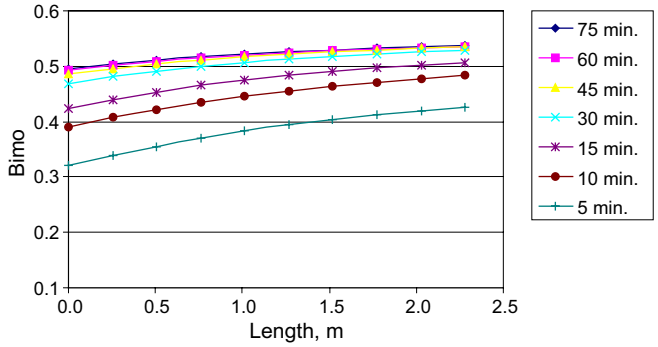

Fig. 10. Variation of Biot number on the inner surface of middle tube along the length of the HTTHE with time.

work the density of fouling deposits is assumed to be constant, whereas the earlier researchers have reported a change in the density and thermal conductivity with temperature [20–23].

The variation of the Biot number on the outer surface of the inner tube (i.e. Bi_{mi}) and on the inner surface of the middle tube (i.e. Bi_{mo}) along the length of the heat exchanger with time are shown in Figs. 9 and 10, respectively. The values of Bi_{mi} are found to be increasing along the length of the heat exchanger during the early period of operation, since T_{d1} and T_{d2} are the same as the constant wall temperature but the bulk fluid temperature increases along the length of the heat exchanger and so do the fouling thickness and Biot numbers. Beyond 30 min T_{d1} and T_{d2} approach towards the bulk fluid temperature and there is only a little difference in the fouling deposit at the inlet and the outlet; hence the Biot number also shows a similar trend as the fouling deposition thickness. The Biot number can be called the dimensionless local fouling factor.

7. Conclusion

The paper presents an improved simulation model, which can be used to predict the fouling thickness and the milk outlet temperature very close to the experimental value. These results once again establish that fouling is controlled by temperature and shear stress on the surface of the heat exchanger. Dimensionless fouling factor in the form of the Biot number can be used in the modeling and simulation of milk fouling. Further for accuracy real time estimation of the heat transfer coefficient is a must and properties of fluids (steam and milk) and deposit should be used as temperature dependent parameters as far as possible. The results are quite encouraging and suggest further scope for technological improvement in the heat treatment of milk in a helical triple tube heat exchanger. The present work is also useful in the modeling for predicting the steam temperature or pressure rise required for controlling the drop in the milk outlet temperature as affected by fouling in a tubular heat exchanger [10]; therefore it can be used for any commercial UHT milk sterilizers with suitable modifications.

References

[1] Santos Olga, Tommy Nylander, Roxane Rosmaninho, Gerhard Rizzo, Stergios Yiantsios, Nikolaos Andritsos, Anastasios Karabelas, H.M. Steinhagen, Luis Melo, L.B. Petermann, C. Gabet, A. Braem, C. Tragardh, M. Paulsson, Modified stainless steel surfaces targeted to reduce fouling-surface characterization, J. Food Eng. 64 (2004) 63–79.

[2] P.J.R. Schreier, P.J. Fryer, Heat exchanger fouling: a model study of the scale up of laboratory data, Chem. Eng. Sci. 50 (8) (1995) 1311–1321.

[3] K.R. Swartzel, Tubular heat exchanger fouling by milk during UHT processing, J. Food Sci. 48 (1983) 1507–1511, 1557.

[4] F. Delplace, J.C. Leuliet, D.A. Levieux, Reaction engineering approach to the analysis of fouling, J. Food Eng. 34 (1997) 91–108.

[5] J. Yoon, D.B. Lund, Magnetic treatment of milk and surface treatment of plate heat exchangers: Effects on milk fouling, J. Food Sci. 59 (5) (1994) 964–969.

[6] B.J. Reitzer, Process design and development, Ind. Eng. Chem. 3 (1964) 345.

[7] Md.I.A. Ansari, M. Sharma, A.K. Datta, Milk fouling simulation in a double tube heat exchanger, Int. Comm. Heat Mass Transfer 30 (5) (2003) 707–716.

[8] P.K. Sahoo, I.A. Ansari, A.K. Datta, Milk fouling simulation in helical triple tube heat exchanger, J. Food Eng. 69 (2005) 235–244.

[9] P.K. Sahoo, Md.I.A. Ansari, A.K. Datta, A computer based iterative solution for accurate estimation of heat transfer coefficients in a helical tube heat exchanger, J. Food Eng. 58 (3) (2003) 211–214.

[10] P.K. Nema, A.K. Datta, A computer based solution to check the drop in milk outlet temperature in a helical triple tube heat exchanger, J. Food Eng. 71 (2) (2005) 133–142.

[11] R. Ranjan, A.K. Datta, Milk fouling simulation in tubular heat exchanger, in: Proceedings 26th National Conference on Fluid Mechanics and Fluid Power, IIT Kharagpur, 1999, 369–374.

[12] P.K. Sahoo, Md.I.A. Ansari, A.K. Datta, Computer-aided design and performance evaluation of an indirect type helical tube ultra-high temperature (UHT) milk sterilizer, J. Food Eng. 51 (1) (2002) 13–19.

[13] C.A. Zuritz, On the design of triple concentric tube heat exchangers, J. Food Process Eng. 12 (1990) 113–130.

[14] N.P. Chopey, T.G. Hicks, Handbook of Chemical Engineering Calculations, McGraw-Hill Book Co., 1984 (Chapter 7, 33).

[15] C.J. Geankoplis, Transport Processes and Unit Operations, third ed., Prentice Hall of India Pvt. Ltd., New Delhi, 1997, 239.

[16] D.Q. Kern, Process Heat Transfer, McGraw-Hill International, New York, 1984, pp. 263–269.

[17] A. Acrivos, Method of characteristics technique – Application to heat and mass transfer problems, Ind. Eng. Chem. 48 (1956) 703–710.
[18] P.J. Fryer, N.K.H. Slater, A direct simulation procedure for chemical reaction fouling in heat exchangers, Chem. Eng. J. 31 (1985) 97–107.
[19] P.J. Fryer, N.K.H. Slater, Control of heat exchangers in the presence of chemical reaction fouling, Chem. Eng. Sci. 41 (1986) 2363.
[20] K. Grijspeerdt, L. Mortier, J. De Block, R.V. Rentergham, Application of modeling to optimize ultra high temperature milk heat exchangers with respect to fouling, Food Control 15 (2) (2003) 117–130.
[21] F. Delplace, J.C. Leuliet, Modeling fouling of a plate heat exchanger with different flow arrangements by whey protein solutions, Trans. Inst. Chem. Eng. 73 (C) (1995) 112–120.
[22] T.J. Davies, S.C. Hentstridge, C.R. Gillham, D.I. Wilson, Investigation of whey protein deposit properties using heat flux sensors, Trans. Inst. Chem. Eng. Food Bioprod. Proc. 75 (C2) (1997) 106–110.
[23] P. Walstra, T.J. Geurts, A. Noomen, A. Jellema, M.A.J.S. Boekel, Dairy Technology, Principles of Milk Properties and Processes, Marcel Dekker, New York, 1999.